RESEARCH ARTICLE

CrossMark

Groundwater vulnerability assessment in karstic aquifers using COP method

Somayeh Bagherzadeh [1] · Nasrollah Kalantari [2] · Amir Fadaei Nobandegani [3] · Zahra Derakhshan [4,5] ·
Gea Oliveri Conti [6] · Margherita Ferrante [6] · Roya Malekahmadi [5]

Abstract

Access to safe and reliable drinking water is amongst the important indicators of development in each society, and water scarcity is one of the challenges and limitations affecting development at national and regional levels and social life and economic activity areas. Generally, there are two types of drinking water sources: the first type is surface waters, including lakes, rivers, and streams and the second type is groundwaters existing in aquifers. Amongst aquifers, karst aquifers play an important role in supplying water sources of the world. Therefore, protecting these aquifers from pollution sources is of paramount importance. COP method is amongst the methods to investigate the intrinsic vulnerability of this type of aquifers, so that areas susceptible to contamination can be determined before being contaminated and these sources can be protected. In the present study, COP method was employed in order to spot the regions that are prone to contamination in the region. This method uses the properties of overlying geological layers above the water table (O factor), the concentration of flow (C factor), and precipitation (P factor) over the aquifer, as the parameters to assess the intrinsic vulnerability of groundwater resources. In this regard, geographical information system (GIS) and remote sensing (RS) were utilized to prepare the mentioned factors and the intrinsic vulnerability map was obtained. The results of COP method indicated that the northwest and the west of the region are highly and very vulnerable. This study indicated that regions with low vulnerability were observed in eastern areas, which accounted for 15.6% of the area. Moderate vulnerability was 40% and related to the northeast and southeast of the area. High vulnerability was 38.2% and related to western and southwestern regions. Very high vulnerability was 6.2% and related to the northwest of the area. By means of the analysis of sensitivity of the model, it was determined that the focus factor of the flow has the greatest impact on the creation of vulnerability in the region. Also, these results were validated through electrical conductivity and discharge time series of the regional springs that are located in the vulnerable zones.

Keywords Groundwater · Karstic aquifer · Vulnerability · GIS

• This study evaluates the vulnerability of Shimbar karstic site using the COP method.
• To validate the inherent vulnerability map obtained by COP method.
• Flow Con. factor is the most effective factor in GW contamination in this study.

✉ Zahra Derakhshan
  d.z.derakhshan1@gmail.com

1 Department of Hydrogeology, Ab Ati Pazhooh Consulting Engineers Company, Shiraz, IR, Iran

2 Department of Geology, School of Earth, Shahid Chamran University, Ahvaz, IR, Iran

3 Department of Environmental Health Engineering, School of Health, Shiraz University of Medical Sciences, Shiraz, IR, Iran

4 Department of Environmental Health, School of Health, Larestan University of Medical Sciences, Larestan, Iran

5 Environmental Science and Technology Research Center, Department of Environmental Health Engineering, Shahid Sadoughi University of Medical Sciences, Yazd, Iran

6 Environmental and Food Hygiene Laboratories (LIAA) of Department of Medical Sciences, Surgical and Advanced Technologies "G.F. Ingrassia", Hygiene and Public Health, University of Catania, Catania, Italy

Introduction

In recent years, due to increased water use, increased constraints, and the high costs of surface water resource development and on the other hand, owing to the aquifers and groundwaters less potential for contamination and their large storage capacity compared to surface waters, groundwaters are regarded as the main sources of water supply in arid and semi-arid regions such as Iran, namely Khuzestan Province (Fazeli et al. 2011; Sha'bani 2008). Amongst aquifers, karstic ones play an important role in supplying the drinking water in Khuzestan Plain in a way that most drinking water supply wells are located in this type of aquifer. Karstic aquifers are also important worldwide because they supply more than 25% of consumed drinking water. In the USA and Europe, 35 and 40% of the water are supplied from karstic resources, respectively. This figure exceeds 50% in Austria and Australia (Biondic and Bakalowicz 1975; Vías et al. 2006).

According to Ford and Williams (2013), karst refers to a region with certain hydrogeology and geomorphology created by rocks with high solubility and well-developed secondary porosity. They believe that karsts are created by dissolution in paths controlled by structural phenomena. In many areas of the earth (usually where carbonate rocks are located beneath the surface), features occur widely and poorly as karst. These karst features are a result of bedrock dissolution.

Characteristics of karst features include:

- Closed sink, swallow holes in different dimensions and shapes
- The existence of seams and gaps as surface drainage
- Caves and underground drainage systems (Ford and Williams 2013)

According to the above-mentioned properties, karstic aquifers consist of interconnected channels (karstic networks) feeding underground drainage (Jeannin et al. 2013). Beside the high significance of karstic aquifers and need for them, their high vulnerability and easy of being contaminated are challenges regarding their sustainable management. The reasons for their high vulnerability include the thin soil cover, the flow concentration in epikarst zone, and concentrated infiltration through karstic porosities. Moreover, the residence time in karstic aquifers is much shorter compared to non-karstic ones. This means contaminants move through them faster and more easily; therefore, the storage capacity in the drainage system is low and natural processes like absorption, degradation, and filtration will have limited effects on the contaminants. Therefore, contamination can reach GW easily and travel inside karstic conduits quickly for long distances (Goldscheider et al. 2000; Polemio et al. 2009). Identifying zones that are prone to contamination and preventing them from being contaminated can help managers and authorities.

Vulnerability is based on the idea that some areas are more sensitive than others with respect to groundwater contamination (Moratalla et al. 2011), and preparing vulnerability maps is a robust and low-cost method capable of playing a key role in determining aquifers which are susceptible to contamination.

Margat (1968) expressed the term "groundwater vulnerability to contamination" for the first time; "vulnerability to contamination" and "natural protection against contamination" terms are also interchangeably used. High vulnerability indicates low natural protection.

Following that, Vrba and Zaporozec (1994) introduced vulnerability as a qualitative, relative, non-measurable, and non-dimensional feature. They expressed the intrinsic vulnerability and peculiar or especial vulnerability notions. Vulnerability assessment only depends on the natural properties of the region and then on the characteristics of contaminants. COST 620 has offered the following definitions for intrinsic vulnerability and peculiar or especial vulnerability (of course, cited by Daly et al. 2002):

- Intrinsic vulnerability is determined by hydrogeological characteristics of an area and independent of the nature of contaminants.
- Peculiar or especial vulnerability is determined by the characteristics of a especial contaminant (or a group of contaminants) and its relationship with hydrogeological system damage.

In order to protect karst aquifers and based on vulnerability and risk mapping, European Commission set up COST Action 620.

The word "COST" is formed by placing the first letters of the phrase "Cooperation in Science and Technology" beside each other. Fifty-one representatives from 15 European countries participated in this project which commenced in 1997 and ended in 2003 (Zwahlen 2004). The European Water Framework Directive (2000) gave double strength to this project. This organization provides the overall framework for water source management.

The conceptual framework proposed by COST Action 620 for karst groundwater intrinsic vulnerability mapping consisted of four factors, including overlying layers, concentration of flow, precipitation regime, and karst network development. Resource vulnerability maps are obtained by integrating overlying layers, concentration of flow, and precipitation regime. It is necessary to add karst network development factor for source vulnerability mapping (Daly et al. 2002; Goldscheider and Popescu 2004); the goal in resource protection is the groundwater existing in the aquifer, and the goal in source protection is the water existing in wells and springs (Goldscheider 2004).

Different methods have been proposed and implemented in order to evaluate the vulnerability of karstic aquifers and prepare their maps, including GOD (Foster 1987), DRASTIC

(Aller et al. 1987), AVI (Van Stempvoort et al. 1993), SINTACS (Civita 1994), EPIK (Doerfliger et al. 1999; Doerfliger and Zwahlen 1998), REKS (Malik and Svasta 1999), RISKE (Petelet-Giraud et al. 2000), RISKE 2 (Plagnes et al. 2005), PI (Goldscheider et al. 2000), Slovene approach (Ravbar and Goldscheider 2007), KARSTIC (Davis et al. 2002), PaPRIKa (Kavouri et al. 2011), COP, and COP + K (Andreo et al. 2009; Vias et al. 2002). Any of these methods include advantages and disadvantages. However, COP is the method that has been proposed as standard for karstic aquifers in Europe. COP method was proposed to evaluate the vulnerability of carbonate aquifers in the framework of European standard "European COST Action 620." In this method, the collection of groundwater flow (C factor), properties of the layers covering the groundwater surface (O factor), and precipitation on the aquifer (P factor) are employed as the parameters to evaluate the inherent vulnerability of groundwater (Biondic and Bakalowicz 1975; Vías et al. 2006).

In their study entitled, "Proposed method for groundwater vulnerability mapping in carbonate (karstic) aquifers: the COP method," Vías et al. (2006) evaluated the vulnerability of GW in two zones in Southern Spain. They selected "Sierra de Libar" aquifer (a conduit flow system) and "Torremolinoes" aquifer (a diffuse flow system) in order to utilize COP method of evaluating vulnerability. They also validated this method and compared the results with three well-known vulnerability mapping methods such as GOD, AVI, and DRASTIC. By comparing this method and utilizing validation assessment tools (hydrogeological data and tracer tests), they indicated that COP is the most appropriate method to assess the vulnerability of groundwater karstic aquifers. In their study, Dimitriou and Zacharias (2006) investigated the vulnerability of a karstic region in Western Greece using COP method. The results of their study indicated that tectonically active parts of aquifer (faults and fractures are extended) were highly and very vulnerable. They prepared the risk map of the region by combining the maps of land use and vulnerability, based on which they showed that human activities increase the risk of contamination. Polemio et al. (2009) studied the vulnerability of Aqalia karstic aquifers in the southeast of Italy using the methods of GOD, DRASTIC, SINTACS, EPIK, PI, and COP. They also compared these methods. They classified these methods into three groups. GOD is utilized for an extensive vulnerable part of the region. DRASTIC and SINTACS are used for all types of aquifers; especially, DRASTIC is more suitable for karstic ones. The third group includes EPIK, PI, and COP that are specifically designed for karstic aquifers and provide acceptable results especially for carbonate formations that have karstic and hydrogeological terrains, specifically PI and COP. They also stated that

the simplest and most flexible methods are those that consider climatic parameters.

The present study was aimed at evaluating the intrinsic vulnerability of groundwater resources of Shimbar karstic site using COP in GIS environment.

Methods

The context of the study area

Shimbar karstic area (Shirin Bahar) with an area of about 325 km^2 is located in 65 km to the northwest of Masjed Suleiman, Khuzestan Province, Iran (see Fig. 1). The average annual rainfall in the region is 473.5 mm. Shimbar karstic aquifer is a vast aquifer with three sub-basins drained by Spring Dareh-e-Anari, Spring Abshekalo, and Spring Sarhoni, which are respectively located in the south, center, and north of the aquifer That the precise boundary of these sub-basins has not so far been determined. The flow systems in the sub-basins of Spring Dareh-e-Anari and Spring Sarhonis and Spring Abshekalo are respectively conduit and diffuse (Kalantari et al. 2010).

From the lithological viewpoint, the geological formations which outcrop in the studied area are related to the Upper Cretaceous up to the present era, and the Ilam-Seruk limestone formation is considered the oldest of these formations; and in the order of decreasing age, there are Pabadeh-Gurpi Formation (marl and gray shale), Amiran Formation (olive-brown siltstones and sandstone), Kashkan Formation (silt, sandstone, and conglomerate), Talezang Formation (gray to brown limestones), Asmari Formation (sandstone with shale interlayer), Aghajari Formation (sandstone and marl), Quaternary conglomerate, and alluvium deposits of the present day on this formation (Fig. 1).

Most part of the region (about 68%) is covered with karstic limestones (initial Oligocene to Miocene–Asmari Formation), which are developed as a result of secondary porosity caused by tectonic fractures, climatic conditions, and karstification. Amongst karstic features, one can refer to polje (Shelar and Chalemonar), caves, karrenfields, and karst springs (Sarhoni, Dareh-e-Anari, and Abshekalo). The morphology of the regional poljes (Shelar and Chalemonar) indicates that these terrains are created as a result of tectonic activities. Chalemonar Thrust (see Fig. 1) is the most important tectonic fracture in the area, which has caused other poljes and also Dareh-e-Anari to form (Kalantari et al. 2010). Secondary fractures of the area (see Fig. 1) are mostly located within Chalemonar polje and Spring Dareh-e-Anari, which exhibits the highest discharge (an average annual rate of about 2.88 m^3/s). The thickest soil cover in the area is mostly seen in Chalemonar and Shelar poljes, whose thickness is more
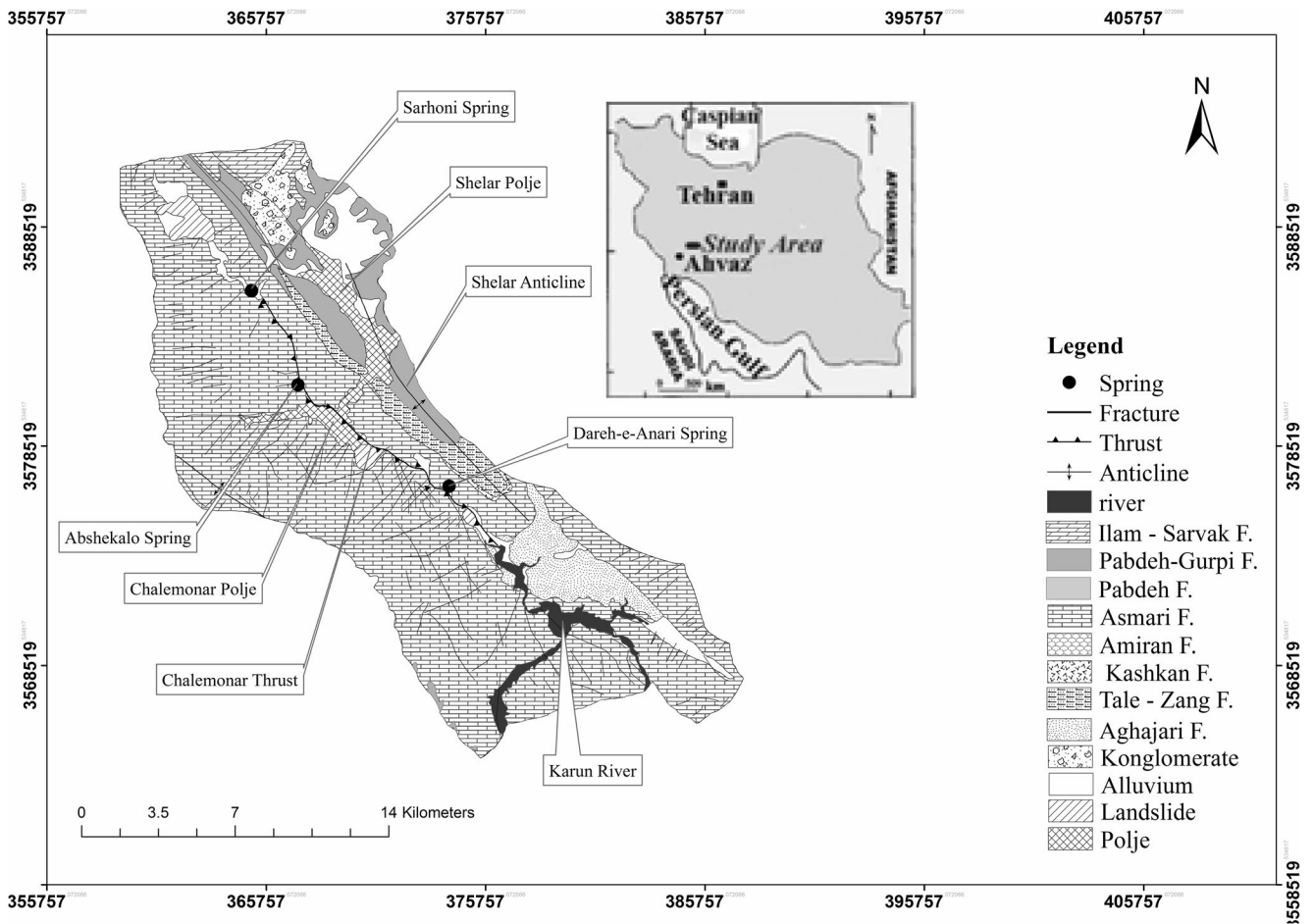
Fig. 1 Location and hydrogeological map of the study area

than 1 m. In other parts of the study area, the soil cover is thin (< 1 m).

Talezang trapped limestone formation is the other permeable formation in the region, but due to limited expansion in the region, its role is low compared with Asmari limestone. Pabadeh-Gurpi and Aghajari formations are of impenetrable outcropped formations in the region.

In the studied karstic region, the trend of dominant fractures is in the direction of northeast-southwest, and most of the fractures are of transverse ones and are vertical on the axis of fold, thus causing more permeability of the hard formations in the region, which is important in terms of hydrogeology.

Preparation of COP factors

COP method includes three main factors: concentration of flow (C), overlying layers (O), and precipitation (P).

Concentration of flow (C factor)

It indicates whether the infiltration water directly and centrally passes the unsaturated zone and enters the aquifer through surface karstic terrains such as shallow holes, sinkholes, or

fractures. This causes an increase in vulnerability of the aquifer. Here, the slope and vegetation of the aquifer can have their impacts. Concentration of flow in karstic aquifer is expressed through two different scenarios according to the hydromorphological conditions of the aquifer:

Scenario 1: It describes a condition in which the basin is covered with low-permeability layers in which the surface runoff enters the swallow holes or surface features that create focused permeability. When both autogenic and allogenic basin feedings flow into the karstic feature, they result in a shortcut in the flow in the unsaturated zone. Evaluating C factor in this scenario includes four variables: the distance to the swallow hole (dh), the distance of to the stream/river (ds), the effect of slope (s), and vegetation (v). The vulnerability of the aquifer decreases with an increase in the distance between the feeding zone and the swallow hole or the stream/river (see Fig. 2). Vegetation (v) includes a percentage of the basin area causes runoff infiltration. The zone with 20–30% vegetation is considered as

a zone with low vegetation. Combining the parameters of vegetation and slope creates a value for the parameter of slope of vegetation (*sv*). As indicated in Fig. 2, in high slopes and low vegetation, vulnerability increases by giving the value near to 1 for the parameter of *sv*. This means that easier infiltration occurs and flows toward the swallow holes and thus shorter travel time to the water table will result.

In this infiltration condition, the rate of *C* factor is calculated by multiplying the obtained values for the parameter of *sv* in the distance between the feeding zone and the shallow hole (*dh*) and the distance between the feeding zone to the subducted river (*ds*) (see Eq. 1).

$$C \text{ factor rate} = dh \cdot ds \cdot sv \tag{1}$$

Scenario 2: This scenario indicates the zones in which only autogenic infiltration occurs. The rate of the *C* factor in this condition is evaluated by combining three variables: surface feature (*sf*), slope (*s*), and vegetation (*v*). Surface feature parameter is amongst those geomorphologic forms which are specific to carbonate rocks and is the presence or absence of any overlapping layer (permeable or impermeable) determining the importance of runoff or infiltration processes (see Fig. 2). According to Fig. 2, evaluating the parameter of slope-vegetation is carried out opposed to scenario 1 because in areas without vegetation and also areas with steep slopes, runoff (and contamination potential) can make its way to the aquifer in any way, except in features such as swallow holes. This condition is common in the slopes of carbonate aquifers. In order to calculate the rate of *C* factor in scenario 2, Eq. 2 is employed.

$$C \text{ factor} = (sf) \cdot (sv) \tag{2}$$

where *sf* is the surface feature parameter and *sv* is the slope-vegetation parameter.

In the studied area, after investigation of geomorphological conditions and hydrological conditions as well as field observations, scenario 2 was selected for evaluation of factor c.

According to this scenario, it is required to prepare two maps of surface complications (*sf*) and slope-vegetation (*sv*) to provide a final map of c factor.

Surface feature (*sf*) As shown in Fig. 2, according to scenario 2, the shape of the surface karst is divided into four categories:

1. Well-developed karsts
2. Low-developed karst or a region with non-soluble shapes
3. Crushed carbonate rocks
4. Non-karstic areas

In order to determine surface feature parameters in the Shimbar karstic catchment, ETM+ satellite image Landsat series and also field observations were utilized. First, using satellite imagery and remote sensing science, fractures were extracted and then the errors were removed by visiting the area. There are different methods to specify and extract fractures using digital data processing. One of these methods is using filtering. The processing operation, which we use some of the brightness levels to create an image, is called filtration. In fact, filtering is a kind of variation in spectral values in which the value of each pixel changes compared to its neighbor pixel and creates a new image that can be different to the original image. Important and commonly used filters in remote sensing include low-pass filters, high-pass filters, and band-pass filters (Abshirini 2004).

To apply a filter on an image, a filter box or filter window is considered and to determine the new brightness degree of the pixels, this filter box moves over the entire image and creates a new image. In the present study, edge detection was filtered out to extract fractures at different angles. Eventually, with the field visit and also using the geological map, the existing errors were eliminated and the final map of the fracture was obtained.

According to the obtained results, parts of the Asmari Formation have a plurality and density of karst geomorphologic phenomena of karst and fractures, and as a result, it can be stated that these parts are composed of a developed karstic network. Therefore, parts of the Asmari Formation with a large number of karstic shapes and fractures are located in the category of well-developed karsts. The other parts of the Asmari Formation in which geomorphologic forms have not been developed are in the category of underdeveloped karsts with non-soluble shapes. The limestone formation of Talezang and Ilam Saruk, which are fractured, falls into the category of crushed carbonate rocks. And the rest of the region's formations such as Pabadeh-Gurpi Formations and Aghajari Formation and the present deposits are in the category of non-karstic areas (Fig. 1). Therefore, each of the above categories was assigned a value according to the criteria of Fig. 2 due to the lack, permeability, or non-permeability of the surface layers. Values vary between 0 (the most impact on
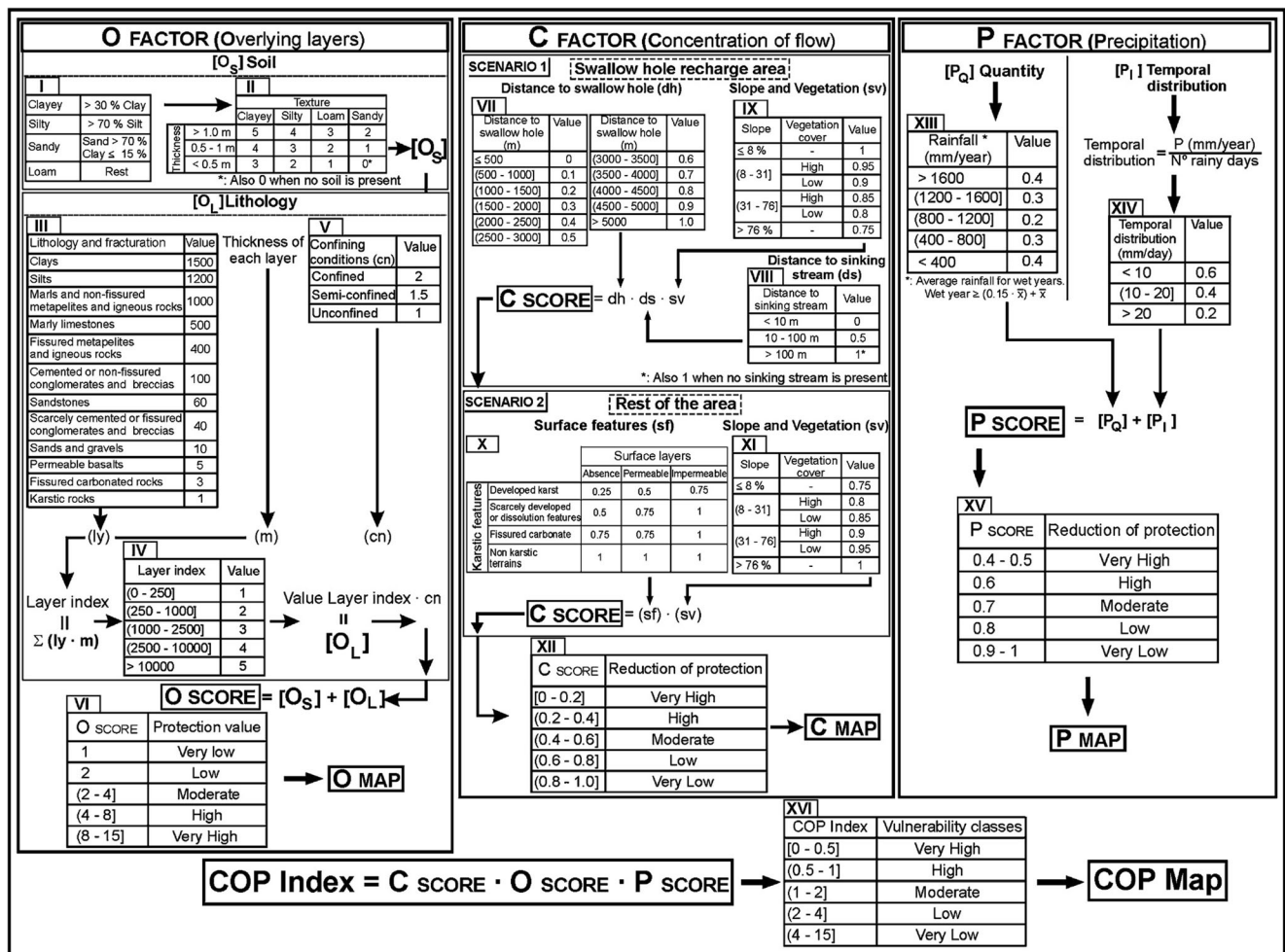
O FACTOR (Overlying layers)

[O_S] Soil

I

Clayey	> 30 % Clay
Silty	> 70 % Silt
Sandy	Sand > 70 % Clay ≤ 15 %
Loam	Rest

II — Texture

Thickness	Clayey	Silty	Loam	Sandy
> 1.0 m	5	4	3	2
0.5 - 1 m	4	3	2	1
< 0.5 m	3	2	1	0*

→ $[O_S]$

*: Also 0 when no soil is present

[O_L] Lithology

III

Lithology and fracturation	Value
Clays	1500
Silts	1200
Marls and non-fissured metapelites and igneous rocks	1000
Marly limestones	500
Fissured metapelites and igneous rocks	400
Cemented or non-fissured conglomerates and breccias	100
Sandstones	60
Scarcely cemented or fissured conglomerates and breccias	40
Sands and gravels	10
Permeable basalts	5
Fissured carbonated rocks	3
Karstic rocks	1

Thickness of each layer (m)

V — Confining conditions (cn)

Confining conditions (cn)	Value
Confined	2
Semi-confined	1.5
Unconfined	1

IV

Layer index	Value
(0 - 250]	1
(250 - 1000]	2
(1000 - 2500]	3
(2500 - 10000]	4
> 10000	5

Layer index = Σ (ly · m)

Value Layer index · cn = $[O_L]$

O SCORE = $[O_S]$ + $[O_L]$

VI

O SCORE	Protection value
1	Very low
2	Low
(2 - 4]	Moderate
(4 - 8]	High
(8 - 15]	Very High

→ O MAP

C FACTOR (Concentration of flow)

SCENARIO 1 — Swallow hole recharge area

Distance to swallow hole (dh)

VII

Distance to swallow hole (m)	Value	Distance to swallow hole (m)	Value
≤ 500	0	(3000 - 3500]	0.6
(500 - 1000]	0.1	(3500 - 4000]	0.7
(1000 - 1500]	0.2	(4000 - 4500]	0.8
(1500 - 2000]	0.3	(4500 - 5000]	0.9
(2000 - 2500]	0.4	> 5000	1.0
(2500 - 3000]	0.5		

Slope and Vegetation (sv)

IX

Slope	Vegetation cover	Value
≤ 8 %	-	1
(8 - 31]	High	0.95
	Low	0.9
(31 - 76]	High	0.85
	Low	0.8
> 76 %	-	0.75

Distance to sinking stream (ds)

VIII

Distance to sinking stream	Value
< 10 m	0
10 - 100 m	0.5
> 100 m	1*

*: Also 1 when no sinking stream is present

C SCORE = dh · ds · sv

SCENARIO 2 — Rest of the area

Surface features (sf)

X

Karstic features	Surface layers — Absence	Permeable	Impermeable
Developed karst	0.25	0.5	0.75
Scarcely developed or dissolution features	0.5	0.75	1
Fissured carbonate	0.75	0.75	1
Non karstic terrains	1	1	1

Slope and Vegetation (sv)

XI

Slope	Vegetation cover	Value
≤ 8 %	-	0.75
(8 - 31]	High	0.8
	Low	0.85
(31 - 76]	High	0.9
	Low	0.95
> 76 %	-	1

C SCORE = (sf) · (sv)

XII

C SCORE	Reduction of protection
[0 - 0.2]	Very High
(0.2 - 0.4]	High
(0.4 - 0.6]	Moderate
(0.6 - 0.8]	Low
(0.8 - 1.0]	Very Low

→ C MAP

P FACTOR (Precipitation)

$[P_Q]$ Quantity

XIII

Rainfall * (mm/year)	Value
> 1600	0.4
(1200 - 1600]	0.3
(800 - 1200]	0.2
(400 - 800]	0.3
< 400	0.4

*: Average rainfall for wet years. Wet year ≥ $(0.15 \cdot \bar{x}) + \bar{x}$

$[P_I]$ Temporal distribution

Temporal distribution = $\dfrac{P \ (\text{mm/year})}{N^{\circ} \ \text{rainy days}}$

XIV

Temporal distribution (mm/day)	Value
< 10	0.6
(10 - 20]	0.4
> 20	0.2

P SCORE = $[P_Q]$ + $[P_I]$

XV

P SCORE	Reduction of protection
0.4 - 0.5	Very High
0.6	High
0.7	Moderate
0.8	Low
0.9 - 1	Very Low

→ P MAP

COP Index = C SCORE · O SCORE · P SCORE

XVI

COP Index	Vulnerability classes
[0 - 0.5]	Very High
(0.5 - 1]	High
(1 - 2]	Moderate
(2 - 4]	Low
[4 - 15]	Very Low

→ COP Map

Fig. 2 Diagram of the COP method, showing the differentiation of the *C*, *O*, and *P* factors (Vías et al. 2006)

vulnerability) and 1 (the least impact on vulnerability). Figure 3 shows the map of the surface complications of the studied area. As seen in the figure, the least value is related to the parts of the region in which the process of carcification has been developed and the geomorphological forms are abundant and the highest value is related to the non-karstic regions.

Therefore, the study area was classified into well-developed bare karstic regions, scarcely developed karstic regions, fissured bare carbonate rocks, scarcely developed karst, which is covered with impermeable layers, and other non-karstic terrains (see Table 1).

Slope-vegetation (*sv*) To prepare the slope-vegetation map, first, the slope map was prepared. For preparing map of the slope, DGN maps of the area with a scale of 1/25,000 were used. Initially, DGN maps were converted to text file with X, Y, Z in MICROSTATION_V8 software, and after eliminating the existing errors, digital elevation model (DEM) was prepared and the slope map was extracted from this digital model. Then, the obtained slope map was provided according to Fig. 2, classification and final map of the slope of the region. Afterwards, the vegetation map of the area was prepared using satellite images and NDVI index.

NDVI or normalized difference vegetation indices are obtained by the difference in infrared banding data relative to the red band, divided by their total. The NDVI range is between − 1 to 1+. When the Earth's surface has no green plant, the value of this index is 0, and as soon as the plants begin to grow, the value of this index increases in the positive direction (Abshirini 2004).

In order to evaluate the vulnerability of karstic areas, the vegetation of the region should be considered qualitatively.
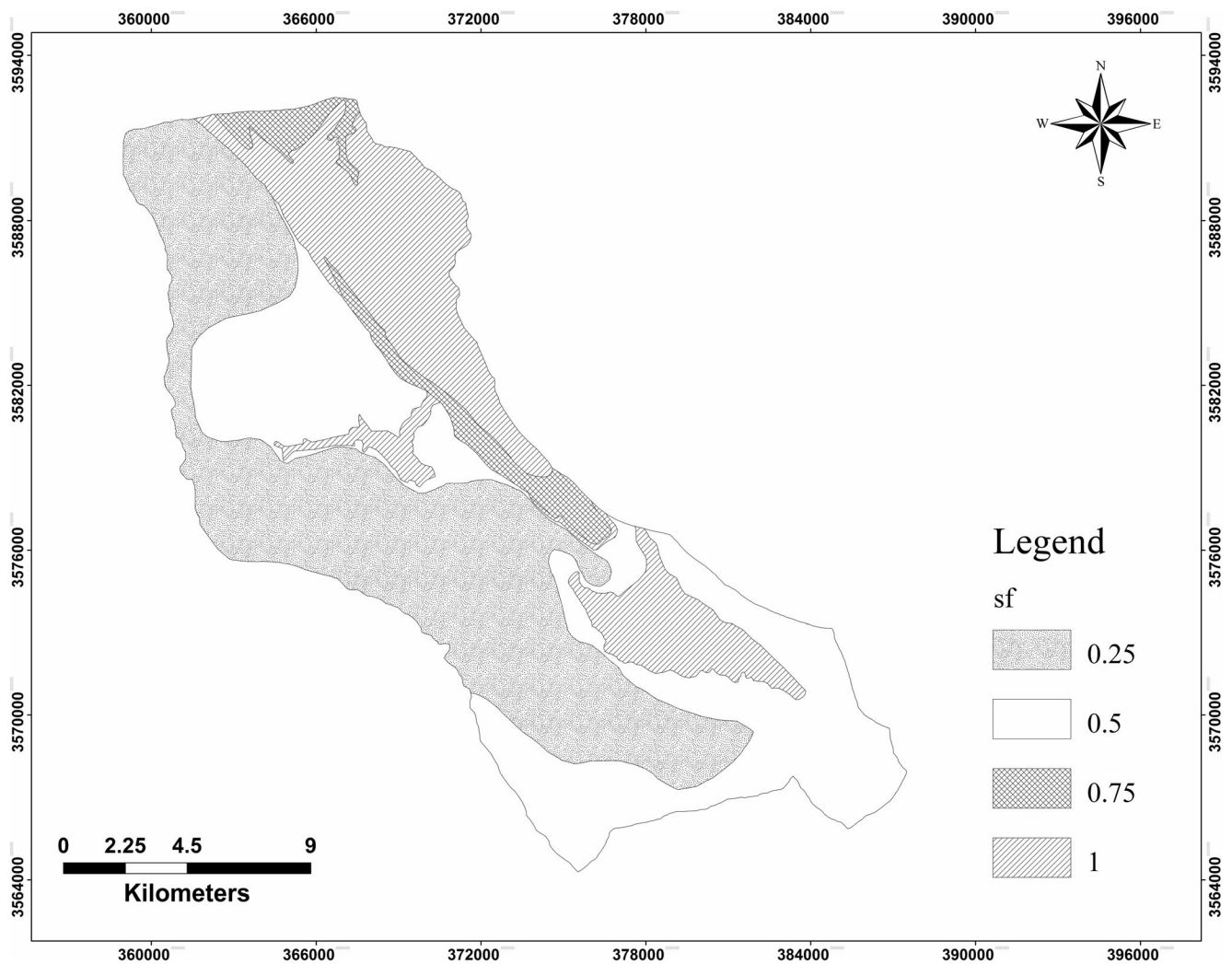
Fig. 3 Surface feature (*sf*) map in Shimbar karstic site

For this purpose, by using ENVI 4.0 software and also NDVI index, vegetation was classified into two classes: with high vegetation class and with low vegetation class.

Also, in order to prepare the slope-vegetation (*sv*) map, the two maps of vegetation and slope were combined and they were valued. According to Fig. 2, areas with a slope of less than 8% regardless of vegetation have the lowest value (0.75) and areas with a slope of more than 76% regardless of vegetation have the highest value (1). Areas with a slope range between 8 and 76% are valued according to vegetation class. Figure 4 shows the slope-vegetation map (*sv*) of the studied area. Finally, the flow concentration map (*C* map) was calculated through Eq. (2).

The factor of overlying layers (factor *O*)

In COP method, only two layers with important hydrogeological role are taken into consideration in order to assess the factor *O*, which include soil (O_S) and lithological layers of the unsaturated zone (O_L) (Vías et al. 2006).

Soil (O_S) This layer includes the top part of the unsaturated soil that continues to the penetration area of the plant roots and the activities of organic creatures (Vías et al. 2006). As indicated in Fig. 2, the soil texture is classified into four groups: clay, silt, sand, and loam. In fact, these textures are an indicator of the soil permeability of the soil. The more the clay percentage of the soil is, the less its permeability will be. Any of these textures have a protection value according to their thickness (see Fig. 2). The highest value is related to the soil that creates the highest level of protection to the aquifer; therefore, a soil that has low permeability and a thickness of over 1 m has the highest protection value, i.e., 5.

In order to prepare the soil map of the studied area, due to the lack of precision of the existing soil map and the lack of well drilling log in the region, soil of the region was sampled, which in general, seven soil samples were prepared. Because of the mountainous nature of the studied area, thick soils were located only in the areas of Chaleh Menar and Shelar plages (seasonal lake bed), which in this area, five specimens were prepared and the other two specimens were prepared from the

Table 1 Values for COP factors and variables in Shimbar site

Factor	Subfactor		Variable		Value
C	Scenario 2:	Surface features	▪ Karst well developed and uncovered		0.25
			▪ Karst scarcely developed and uncovered		0.5
			▪ Fissured carbonate and uncovered		0.75
			▪ Karst scarcely developed covered by a permeable bed		1
			▪ Absence of karst features		1
		Slope and vegetation	▪ ≥ 8%		0.75
			▪ 8–31%	High vegetation	0.80
				Low vegetation	0.85
			▪ 31–76%	High vegetation	0.90
				Low vegetation	0.95
			▪ > 76%		1
O	Soil (O_S)	Texture and thickness	▪ Loam and > 1 m		3
			▪ Loam and 0.5–1 m		2
			▪ Sandy and > 1 m		2
			▪ Loam and < 0.5 m		1
			▪ Non-soil		0
	Lithology (O_L)	Lithology and fracturation	▪ Marls		1000
			▪ Cemented or non-fissured conglomerates		100
			▪ Scarcely cemented or fissured conglomerates		40
			▪ Sands and gravels		10
			▪ Fissured carbonate rocks		3
			▪ Karstic rocks		1
		Confined conditions	▪ Unconfined		1
P	Quantity (PQ)	Average precipitation for wet years	▪ 400–800		0.3
	Intensity (PL)	Precipitation and number of days	▪ 10–20		0.4

thin earth cover (about 30 cm) on karstic Asmari Formation. After analyzing samples by shaker and hydrometric method, the tissue type of each sample was determined. From top to down, soil texture in Chaleh Menar and Shelar plages varies from gravel to sand, and finally to loamy soil. In general, the soil cover of the studied area has loamy texture. After determining the type of soil texture, considering the thickness of the soil in the region according to the criteria of Fig. 2, each specimen was given a value (Table 1). It should be noted that in regions where no soil exists, the value is given zero. Figure 5 shows the soil map (O_S) of the studied region. As seen in the figure, most parts of the studied region are without earth cover, which are rated 0, and there are soil cover with a thickness of more than half a meter is only in the areas of Chale Menar and Shelar plages and also Abeshko Spring, which ranks of 2 and 3 are assigned to them and the areas that ranked 1 are composed of loamy soil with a thickness of less than half a meter (about 30 cm). For Shimbar karstic site, most of the area lack soil cover, and there is loam and sand soil with

thickness of more than 1 m only in the polje areas of Chalemonar and Shelar.

Lithology (O_L) The subfactor of lithology (O_L) reflects the capacity attenuation of each layer of the unsaturated zone. The criteria used to quantify this parameter are as follows: (1) *ly*: indicating the type of rock (hydrogeological characteristics, mainly effective porosity and hydraulic conductivity of the rock) and degree of crushing; (2) the thickness of each layer (*m*); and (3) type of aquifer (*cn*) (Vías et al. 2006). The lithology of each layer in the unsaturated zone is given a value according to Fig. 2. The highest value is related to clay rocks which have a low permeability, and the least value is related to karstic rocks with high permeability. The value given to each lithology of the unsaturated zone layer is multiplied by the thickness of that layer, and in the next step, all layers are summed together according to Eq. (3) and are ranked and valued according to Fig. 2. As stated above, for the determination of the lithology subfactor, the parameter *cn* is also used,
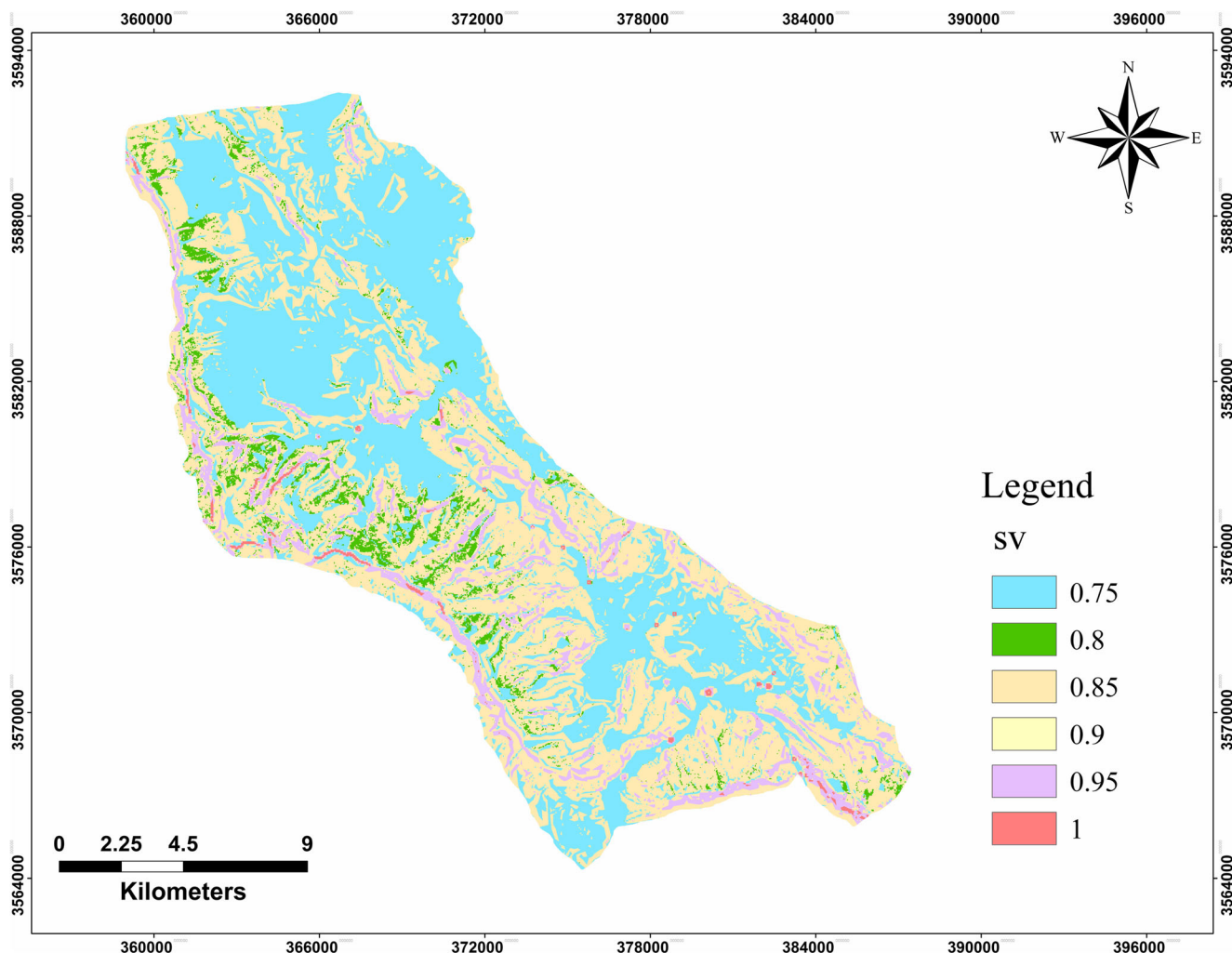
Fig. 4 Slope-vegetation (*sv*) map in Shimbar karstic site

which means that the type of aquifer is determined from the point of view of being captured or free and is valued according to the criteria of Fig. 2. Then, according to Eq. (4), the *cn* rating is multiplied in the layer index and finally lithology subfactor of the unsaturated zone (O_L) layers is calculated.

$$\text{Layer index} = \sum(ly \times m) \qquad (3)$$

where *ly* is the value given to each layer and *m* is the thickness of layer.

$$\text{Value layer index} \cdot cn = O_L \qquad (4)$$

where *cn* is the type of aquifer and O_L is the lithology map of unsaturated zone layers.

In the studied area, using the geological sections (Fig. 6) and also the fact that the aquifer is free, the thickness and sediment of the layers of the unsaturated zone were determined and the lithology map (O_L) was

provided as presented in Fig. 7. According to this figure, the southern parts of the region have a low permeability and the highest value in terms of the lithology subfactor. Finally, the map of the overlying layers (*O* factor) was obtained using Eq. 5.

$$O_{\text{map}} = O_S + O_L \qquad (5)$$

Precipitation factor (factor *P*)

In the COP method, the precipitation factor map (*P* map) is obtained by estimating the rainfall intensity of the study area (PI) and the annual amount of rainfall (PQ).

Precipitation quantity (PQ) An appropriate method to calculate the basin precipitation quantity is drawing iso-rainfall map of the area. Such a map was built, and a map that included the basin and had proper scale and elevation (digital elevation model of precipitation or DRM) was necessary.
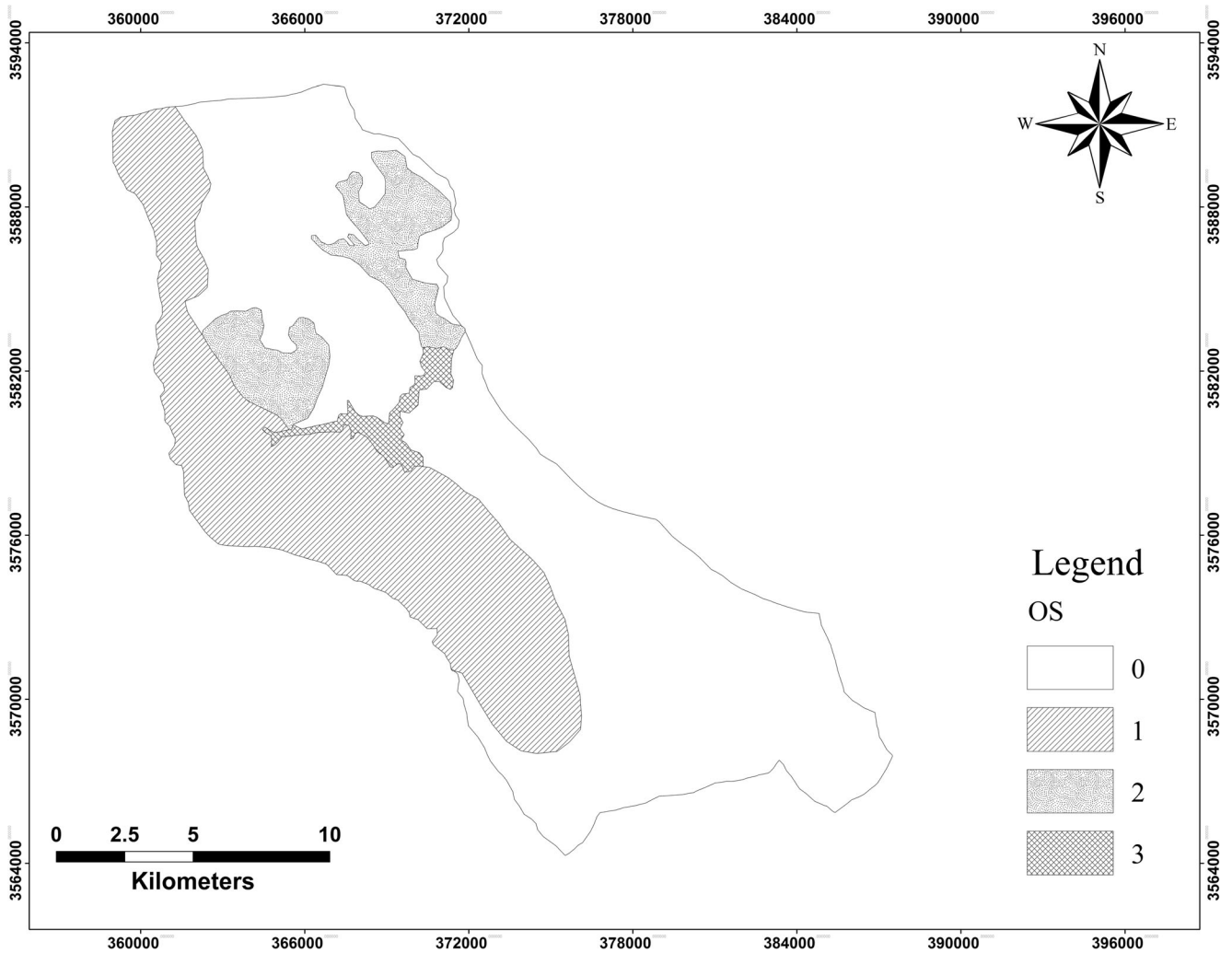
Fig. 5 Soil (O_S) map in Shimbar karstic site

In order to investigate the rainfall gradient, the correlation between height and 10-year mean annual rainfall of the stations has been studied. Due to the limited frequency of rain gauge stations in mountainous areas, it was tried to use some stations outside of the limited area as well. As a result, the elevation and the statistics of the Chelo, Bibi Talkhon, and Shahid Abbaspour stations located in the north, west, and south, respectively, of the studied region, whose position shown in Fig. 8, were used. Based on this, the correlation between height and annual rainfall was extracted (Fig. 9). First, using the DGN maps of the region with a scale of 1:25,000, the DEM of the area was prepared in the GIS environment, then the relationship of annual rainfall gradient (Eq. 6) on the DEM of the studied area was applied and a digital rainfall map (DRM) was prepared and then it was classified and evaluated and the map of rainfall (PQ) was obtained. The precipitation quantity (PQ) for the study area was 400–800 mm/year, which has a value of 0.3 (see Fig. 2).

$$P = 2211.7 \cdot H^{-0.22} \tag{6}$$

in which P is the rainfall (mm), and H is the height (m).

Precipitation temporal distribution (PI) Factor PI considers the precipitation temporal distribution in a certain period of time; therefore, it indicates the precipitation intensity (Sha'bani 2008).

For approximation of this subfactor, two variables are considered for a wet year, including the average annual rainfall and the number of rainy days (Eq. 7). According to Eq. (7), the values assigned to the subfactor of time distribution of rainfall are increased with the increase of the total annual precipitation and the number of rainy days. This causes the feeding and rapid penetration to the karstic tract and gaps to increase and, as a result, increases aquifer vulnerability. If daily precipitation is higher, it makes greater amount of flowing water to run toward the penetration cavities that provide concentrated penetration. Where penetration is slow and of a propagandistic nature, the subfactor PI subtracts. With regard to Fig. 2, it is seen that
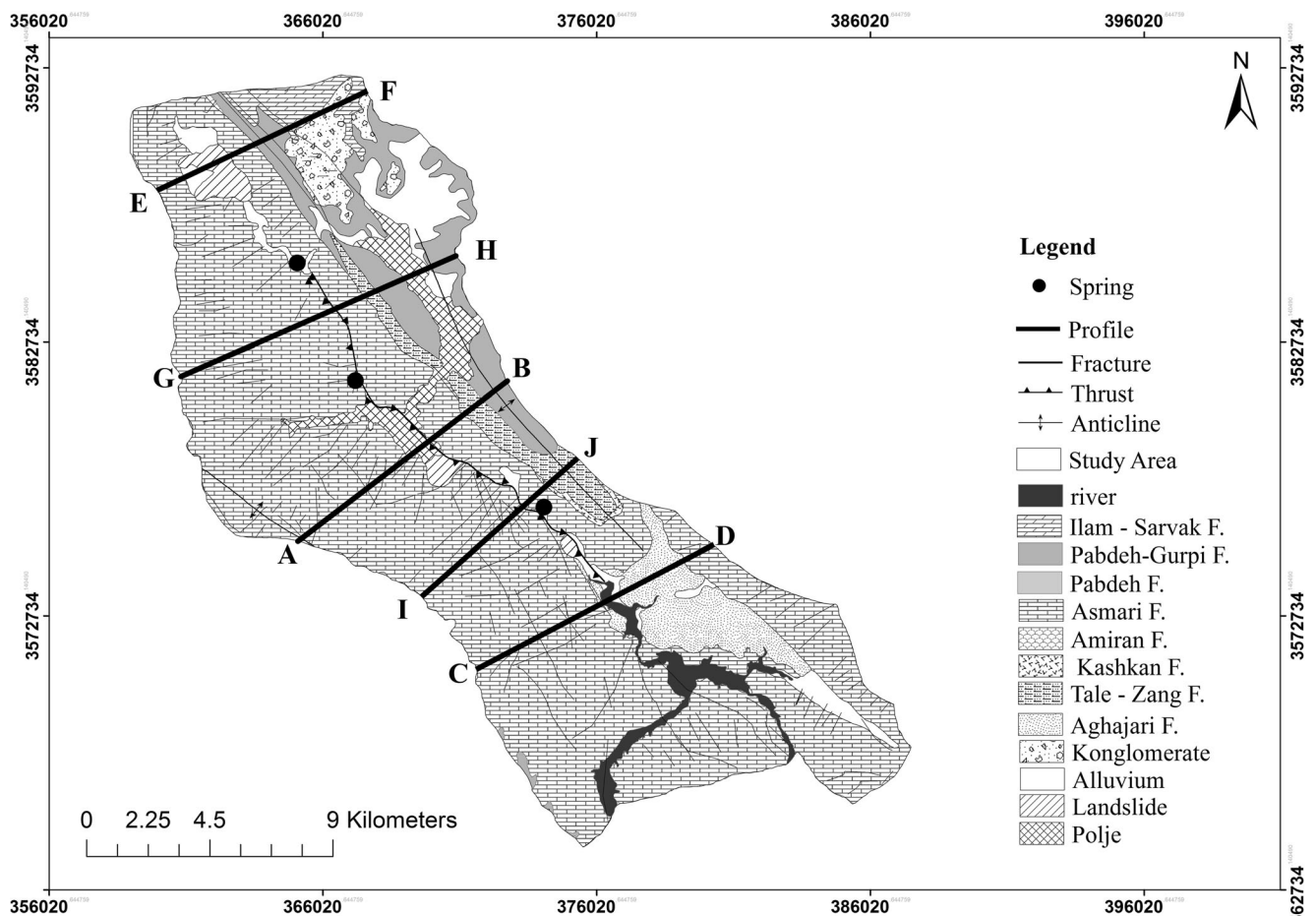
Fig. 6 The geological profile of the studied area

the greater the impact of subfactor PI on the vulnerability, the lower its value; thereby, the value given to it decreases by increasing the time distribution of rainfall (PI).

$$\text{time distribution of rainfall} = \frac{P}{N^\circ} \qquad (7)$$

where P is the average annual precipitation (mm per year) and N° is the number of rainy days.

In order to prepare the time distribution of rainfall map in the studied area, the time distribution of rainfall was calculated for each rain gauge station; and after preparing the database in Excel environment and converting to an acceptable format in the GIS environment, it became point effects and eventually with the interpolation, classification, and valuation, the rainfall distribution map was prepared. The precipitation temporal distribution for the study area was 10–20 mm/day (which has a value of 0.4) (see Fig. 2).

In the last step, by using Eq. (8), two precipitation maps (PQ) and time distribution rainfall (PI) are collected and the map of the precipitation factor is obtained.

$$P_{\text{map}} = PQ + PI \qquad (8)$$

COP index

After the base maps are prepared, the parameters are multiplied by Eq. (9) and the resulting map is classified based on the standards of Fig. 2, and then the COP vulnerability map is obtained.

$$\text{COP} = C \cdot O \cdot P \qquad (9)$$

where C is the flow concentration, O is the cover layer, and P is the precipitation.

In general, the final COP index locates in the range of 0 (very high vulnerability) to 15 (very low vulnerability), which is classified in five groups including: (a) 0–0.5 (very high vulnerability), (b) 0.5–1 (high vulnerability), (c) 1–2 (moderate vulnerability), (d) 2–4 (low vulnerability), and (e) 4–15 (very low vulnerability).
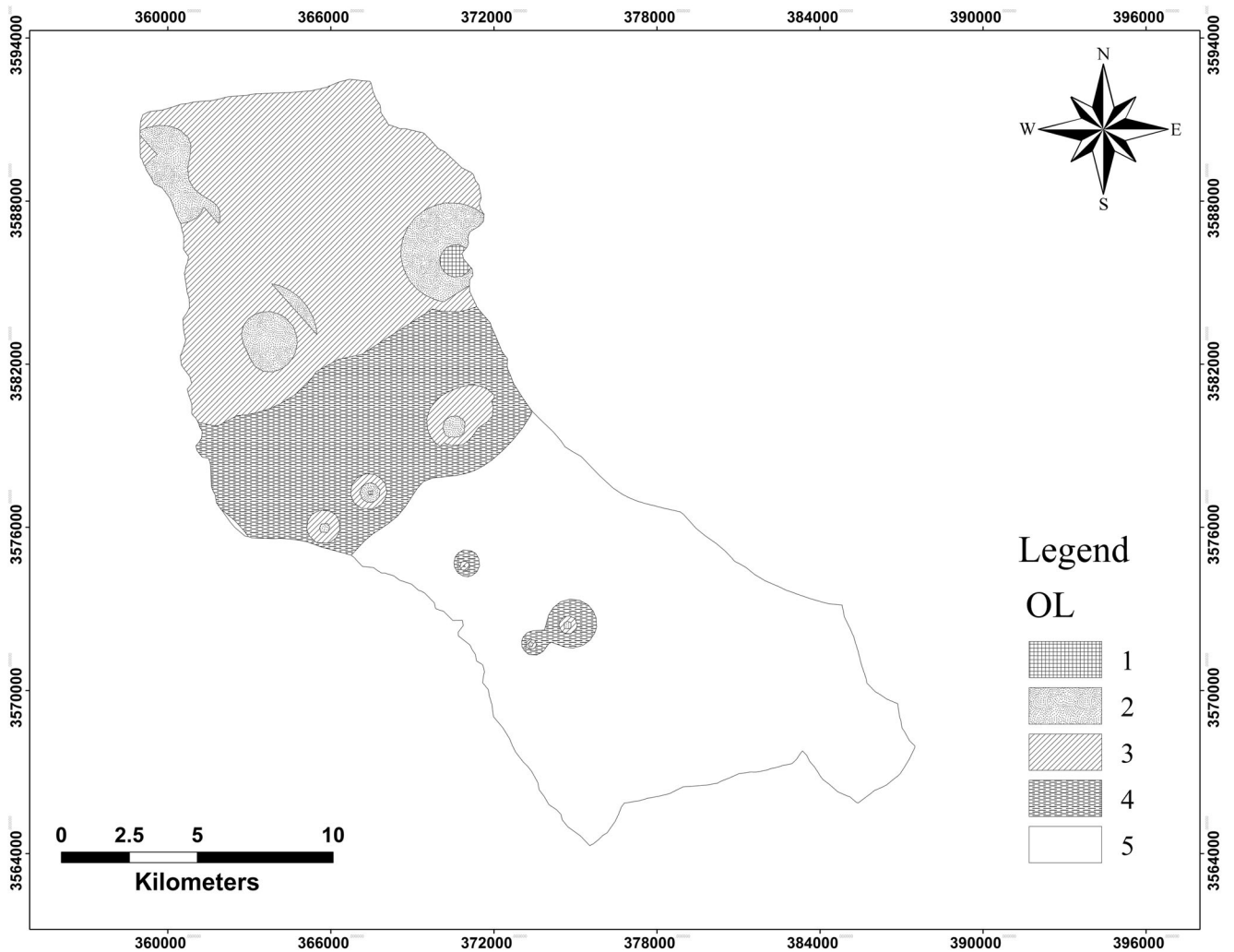
Fig. 7 Lithology (O_L) map in Shimbar karstic site

Results and discussion

Concentration of flow (C factor)

Figure 10 presents the flow concentration (*C* factor) map for Shimbar karstic site. As shown in Fig. 10, in the western part of the region where the Asmari limestone formation is outcropped and has many fractures, the process of carcification has expanded and also this part of the region has more vegetation. Therefore, it has the highest amount of risk of vulnerability in terms of concentrations of flow factor. Also, in the east of the region where the kind of formations is mainly non-calcareous and composed of marl, there is the lowest amount of risk of vulnerability. In general, the factor of flow concentration in most parts of the region has caused a very high, high, and moderate vulnerability risk.

The factor of overlying layers (factor O)

Figure 11 is the final map of overlying layers of the study area. As observed in Fig. 11, the center and the south of the area create a high level of protection against vulnerability of the aquifer. The *O* factor in the south of the aquifer has protected against vulnerability and has created a modest protection in the north of the aquifer, whereas in the small sections in the northeast and the conservation center, it has low protection. So, this factor generally corrects the vulnerability in the studied area.

Precipitation factor (factor P)

According to Fig. 12, the maps of precipitation quantity and precipitation temporal distribution were overlain and the precipitation map was obtained. Precipitation of the study area was moderate (0.7).
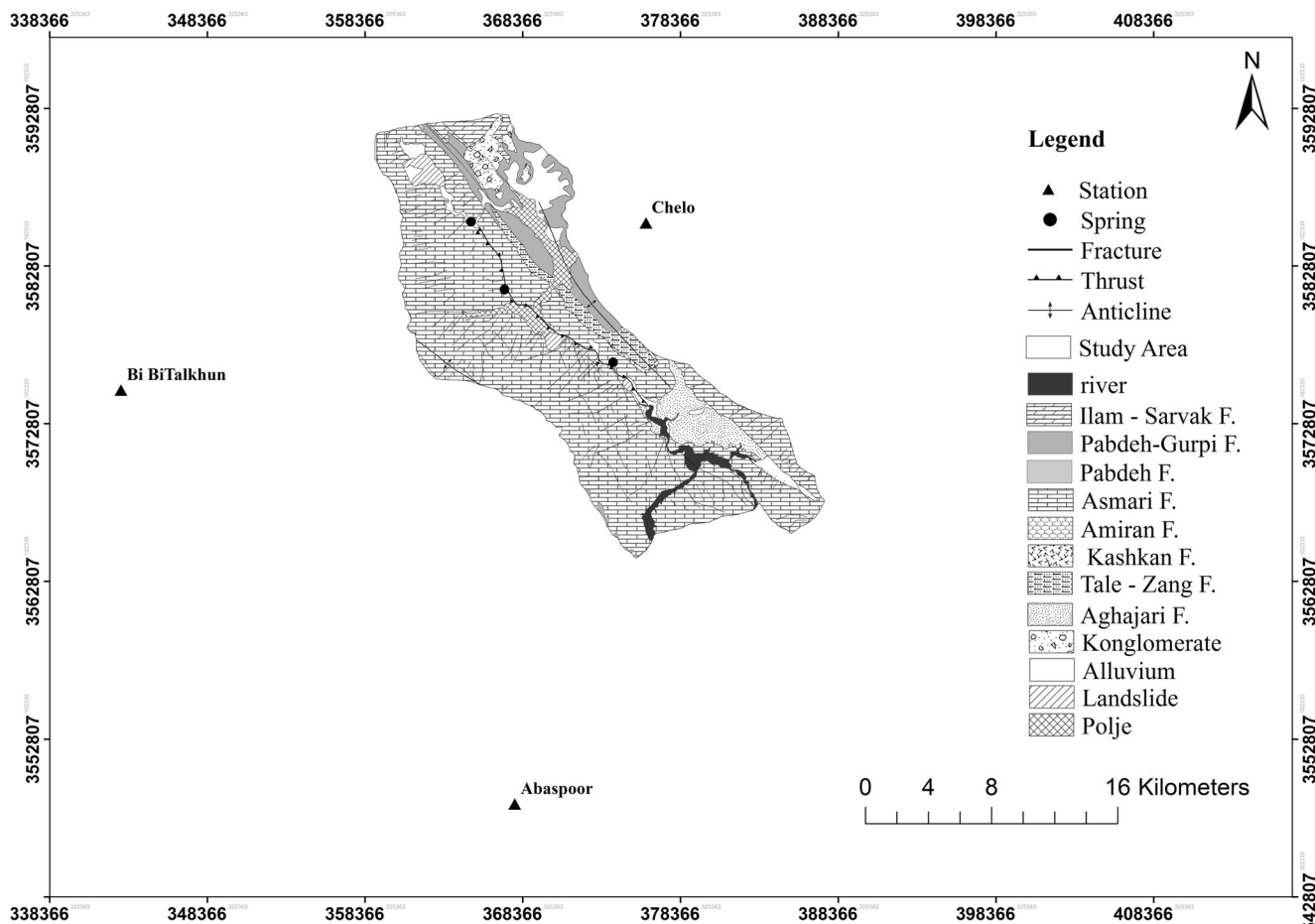
Fig. 8 The situation of the meteorological stations used in this research

Vulnerability of Shimbar karstic aquifer (COP index)

A final intrinsic vulnerability map of Shimbar karstic aquifer was obtained by combining the *C*, *O*, and *P* factor maps (see Fig. 13). The results of COP index for the study area were between 0.26 (minimum) and 4 (maximum), which is classified into four vulnerability classes:

very high, high, moderate, and low. About 6.2% of the area of the region falls in the very high vulnerability class, 38.2% in the high vulnerability class, 40% in the moderate vulnerability class, and 15.6% in the low vulnerability class. The vulnerability map of the area (see Fig. 6) indicates that a small part of the area (northwest) has a very high level of vulnerability, and

Fig. 9 Correlation between height and annual precipitation at three stations: Cheloo, Bibitalkhon, and Shahid Shahid Abbaspour
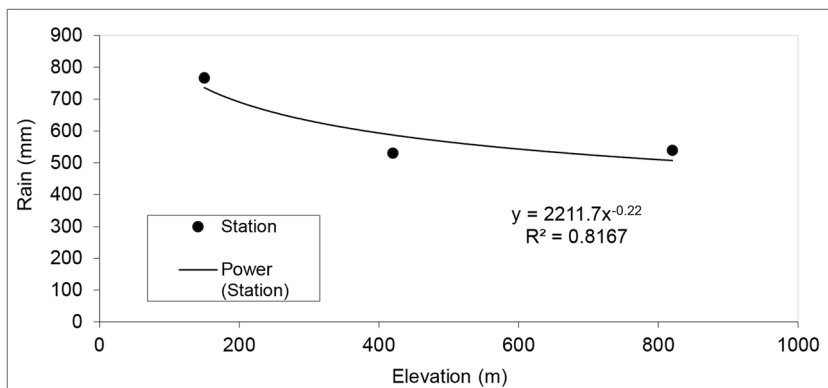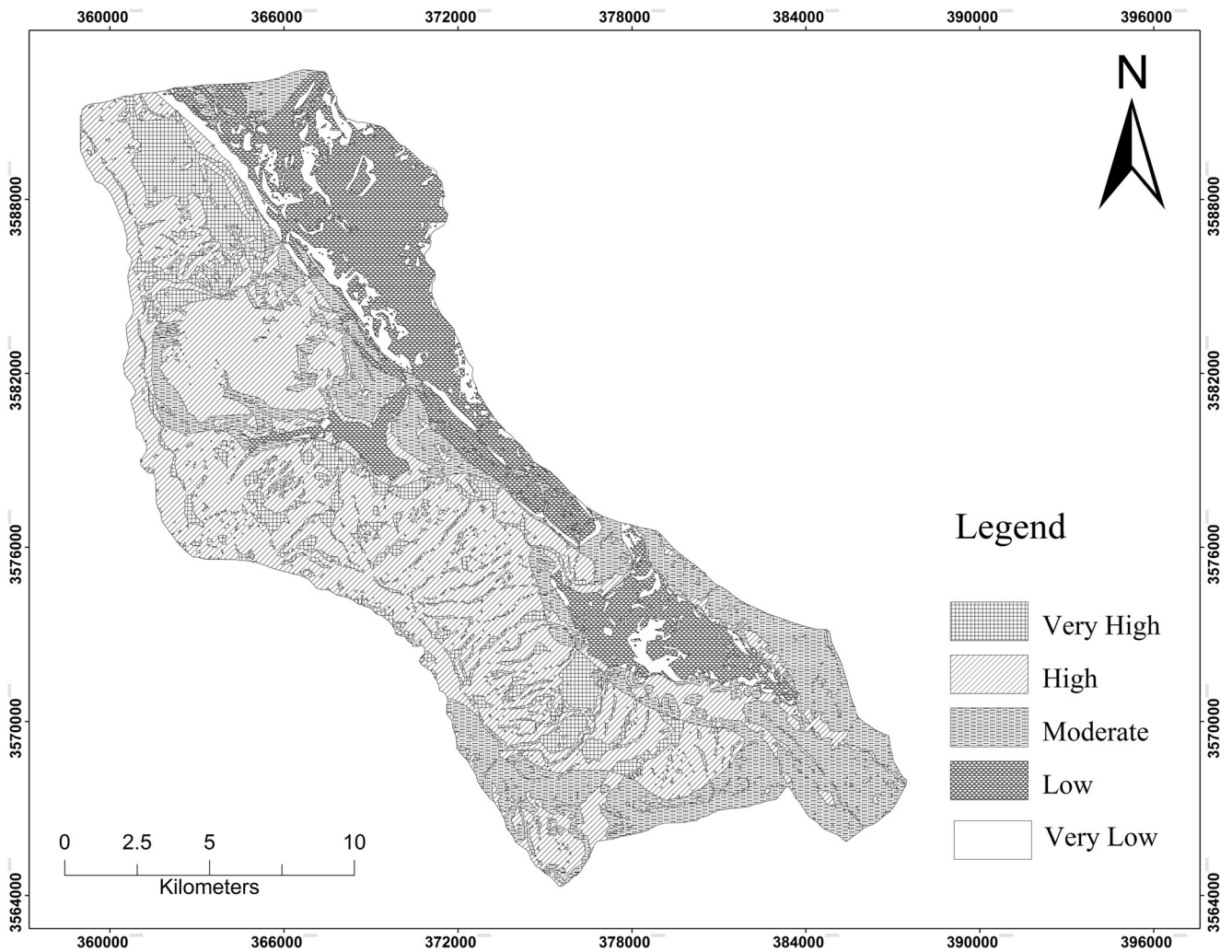
Fig. 10 Flow concentration factor in Shimbar karstic site

the west and the southwest of the area have high vulnerability. The greatest vulnerability of the region has been created in Asmari Formation and karst development due to the development of fractures. Chale Menar and Shelar plages have low vulnerability to pollution due to the thick soil covers and the existence of shale and marl formations of Pabadeh-Gurpi.

Also, in a study constructed by Maryam Naghadizadeh and her colleagues in Izeh Region of Khozestan Province in Iran (Naghdizadegan Jahromi et al. 2013), COP and COP-AHP methods have been tested for vulnerability assessment. The results of the vulnerability maps showed that Asmari limestone formation is more exposed to contamination. Also, by comparing nitrate zoning map as the map of regions' pollution with vulnerability maps, two methods were determined that the vulnerability map obtained from the COP-AHP method has the highest correlation, and as a result, this method could better estimate vulnerability in the region.

Masoompoor Samakosh K and colleagues used the COP method to investigate the vulnerability of the Gilan-e Gharb karstic region in the southwest of Kermanshah Province in western Iran (Masoompour Samakosh et al. 2013). The results of this study showed that the regions formed from Asmari limestone formation have developed karst and these parts have shown a lot of vulnerabilities. In general, most of the region is located in the range of low and medium vulnerability, and flow concentration and precipitation factors have caused reduction of vulnerability in the region, but the factor of the cover layers has caused a lot of vulnerability, which generally vulnerability in the region is low or moderate.

Validation

After vulnerability maps are prepared, it is suggested that their accuracy is validated (Brouyère et al. 2001; Jeannin et al. 2013; Perrin et al. 2004). Different methods have proposed,
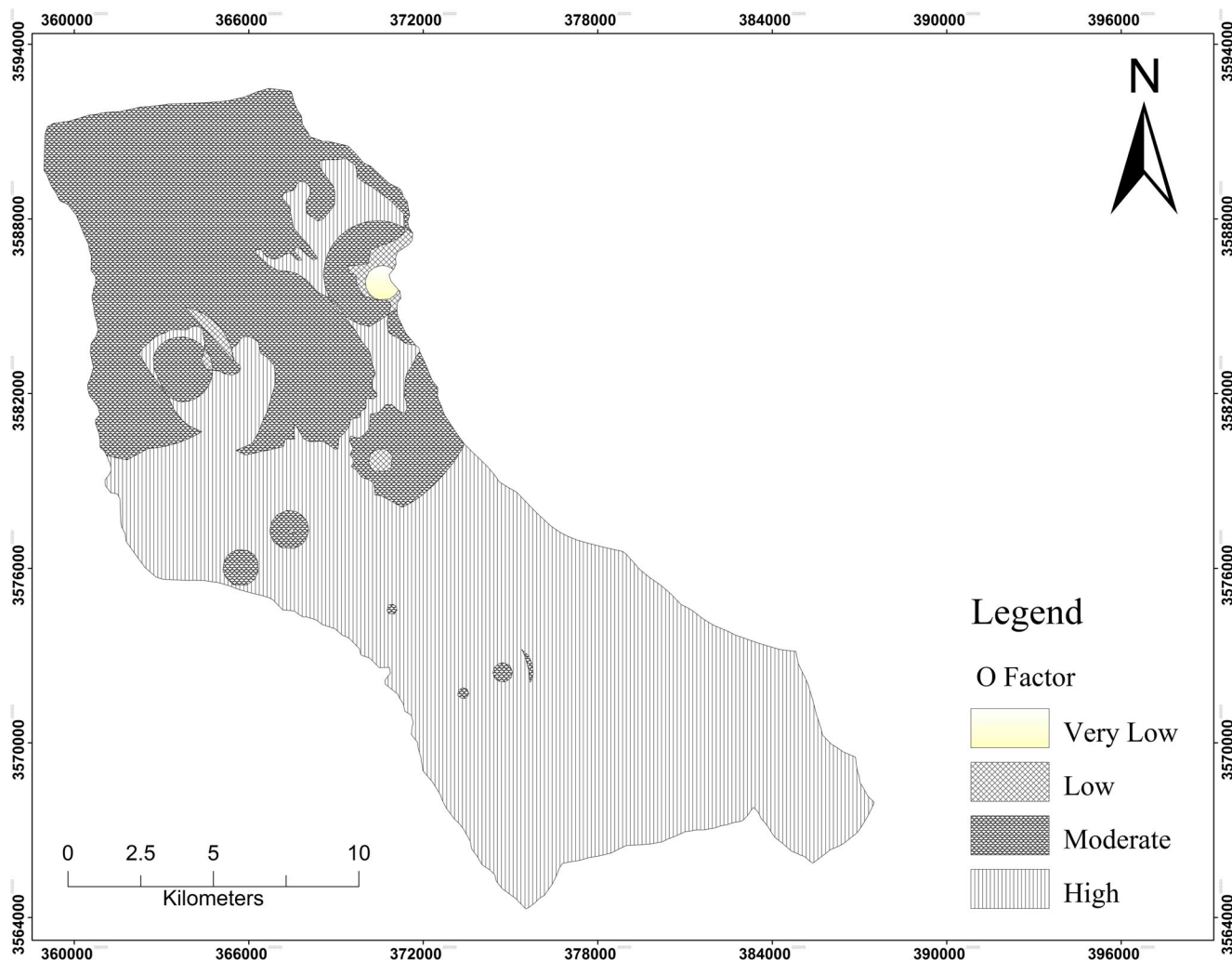
Fig. 11 Overlaying layers factor in Shimbar karstic site

including hydrographs, water chemistry time series, and traces (natural or artificial). Electrical conductivity (EC) time series of the springs were used to validate the regional COP map (see Fig. 14). Results show that infiltration caused by precipitation reaches the springs in a very short time (less than 1 to 2 days after precipitation), which indicates the existence of a very fast flow (from almost 0 to several cubic meters per second). Hydrodynamic response of the aquifer to precipitation reduces the EC of GW resulting from the springs from 370 (Spring Dareh-e-Anari) to 270 μS/cm (Spring Sarhoni). Rapid decrease in EC was observed after each infiltration period, although the lowest EC values were recorded several weeks after the maximum flow rate. This data indicates that hydrochemical response in the springs is caused by the shallow hole basin area and not just point sources (i.e., shallow hole), which indicates different vulnerability classes in this area. The EC time series of Spring Abshekalo also indicated that after the flow increased, EC showed no changes, which indicates that karstification process is less developed in the basin of this spring (see Fig. 14).

Also, water of Dareh-e-Anari and Abshekalo springs was sampled as representatives of the areas with high and medium vulnerabilities (Fig. 13) for testing coliform bacteria (indicating groundwater contamination by surface water), respectively. The results of the test showed (Table 2) that the water of Dareh-e-Anari Spring has coliform bacteria, but Abshekalo Spring lacks these bacteria, and this also confirms the results.

Analyzing the sensitivity of COP model

In Table 3, the statistics summary of the three parameters utilized in COP index calculation is presented. The highest risk of GW contamination is Shimbar karstic aquifer is related to overlaying layers' factor (mean = 4.6), while the flow concentration factor results in less contamination (mean = 0.41). To analyze the sensitivity of COP model, map removal sensitivity analysis, proposed by Lodwick et al. (1990), was applied. This can be calculated through Eq. (10) (Lodwick et al. 1990).
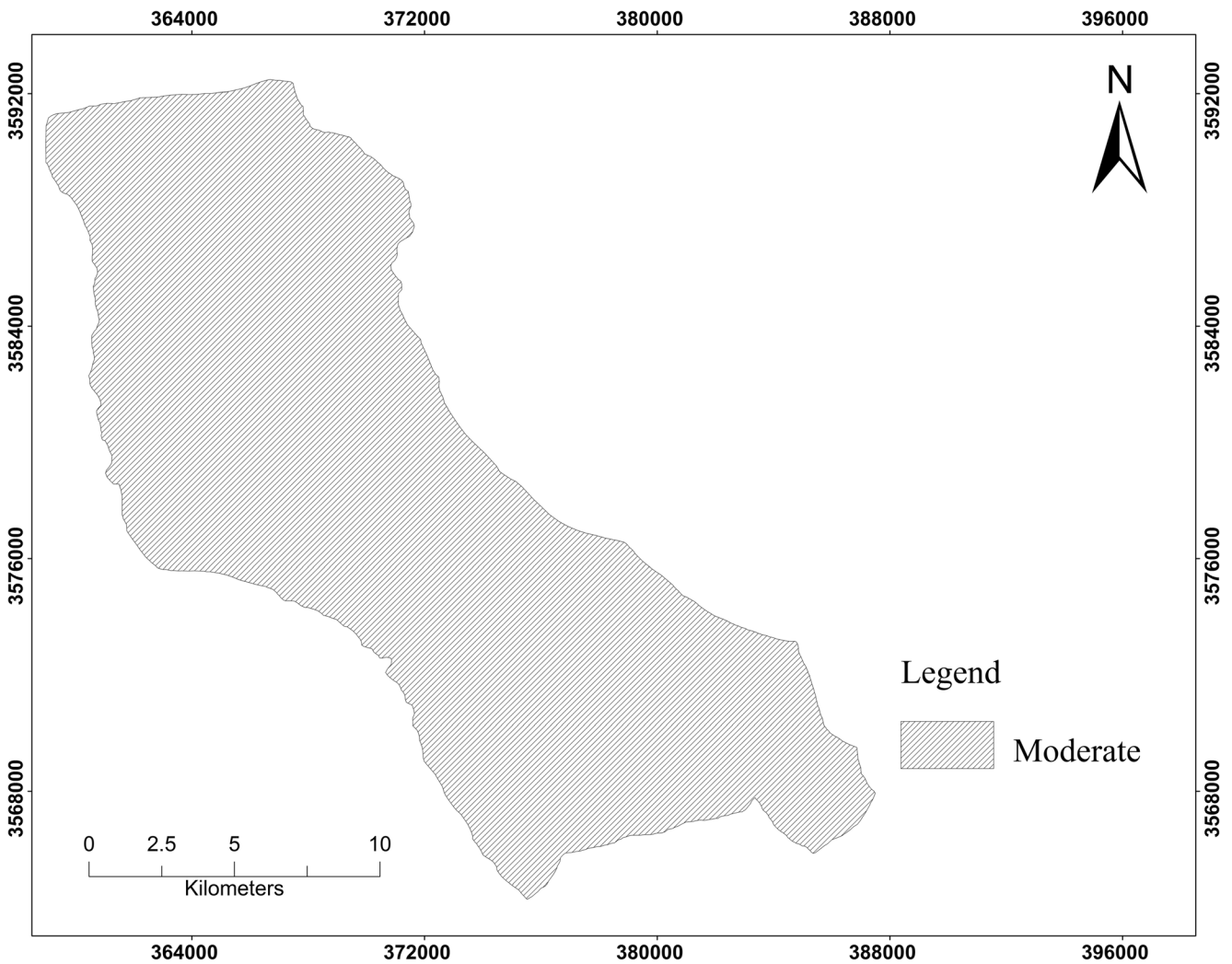
Fig. 12 Precipitation factor in Shimbar karstic site

$$S = \left(\left| V/N - V'/n \right| / N \right) \times 100 \qquad (10)$$

where S is the variation index, V and V' are the unperturbed and the perturbed vulnerability indices, respectively, and N and n are the number of the layer utilized in calculating V and V'. The real index of vulnerability that is calculated using all the parameters is considered as the unperturbed vulnerability index, while the calculated vulnerability using a less number of layers is considered as the perturbed vulnerability. Using this method, one can identify the most effective parameter in GW contamination in the study area. The results of analyzing the sensitivity of map removal (see Table 4) indicate that the mean of variation index of flow concentration (C) factor is more than the other two factors; therefore, it is the most effective factor in GW contamination in the study area.

Conclusion

The present study was conducted in order to evaluate the vulnerability of Shimbar karstic site using COP method and applying GIS and remote sensing software (including flow concentration (C factor), overlaying layers (O factor), and precipitation (P factor)). The results of the study indicate that low vulnerability was observed in eastern areas, which accounted for 15.6% of the area. Moderate vulnerability is related to the northeast and southeast of the area (40%). High vulnerability is related to western and southwestern regions (38.2%). Very high vulnerability is related to the northwest of the area (6.2%). In the area of Shimbar, according to the theory of COP method, in terms of concentration of flow factor (C), the greatest vulnerability of the region has been created in Asmari Formation and karst development due to the development of fractures. The trend of dominant fractures is in the direction of northeast-southwest, and most of the fractures are transverse fractures and are perpendicular to the
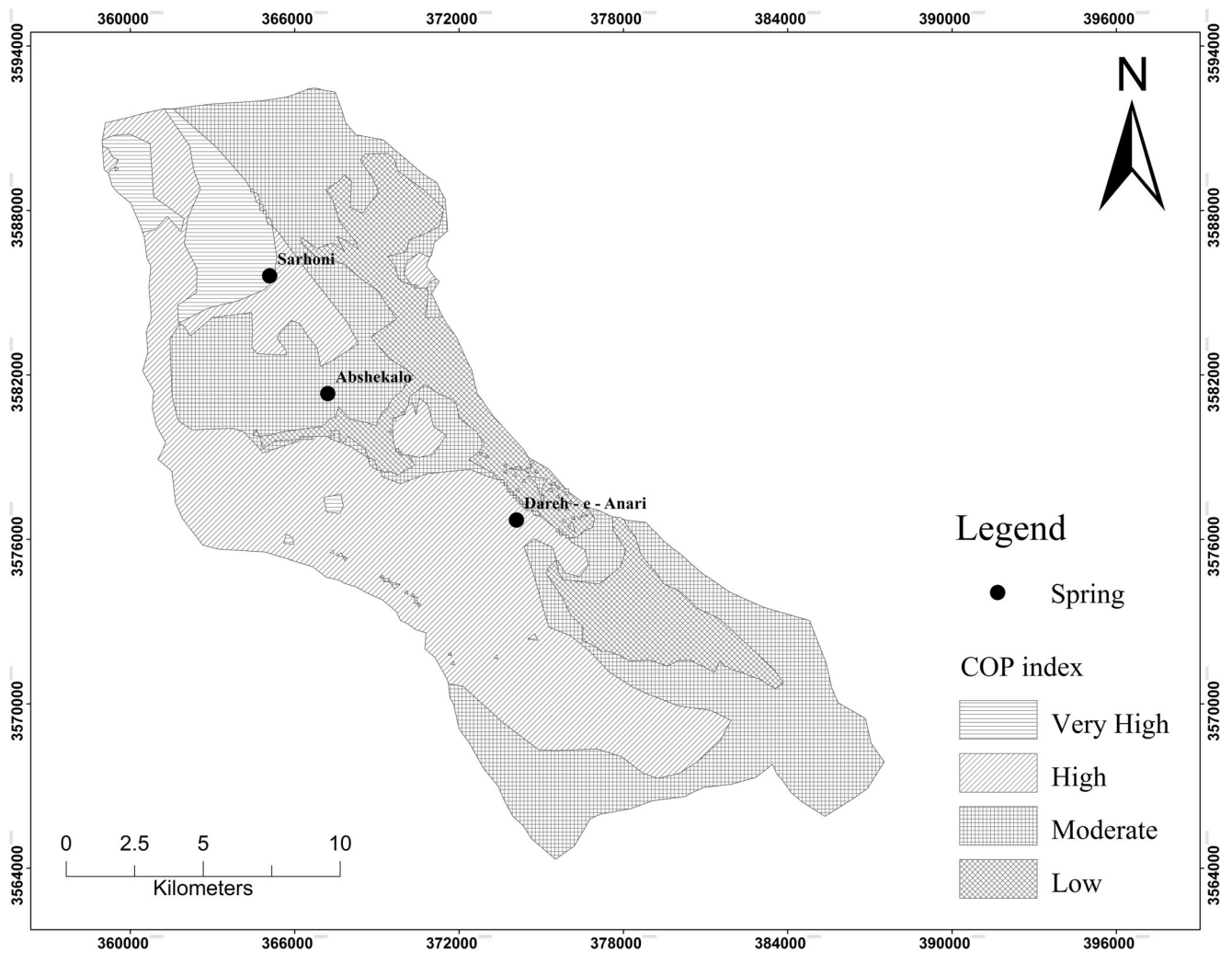
Fig. 13 COP vulnerability map in Shimbar karstic site

axis of fold and thus cause the permeability of most of the hard formations in the region. Also, by analyzing the sensitivity of the model, it was determined that the concentration of flow factor has the greatest impact on the vulnerability of the region. However, in terms of cover layers factor, due to the fact that Marne and Chile formations are expanded in the aquifer's unsaturated zone, the risk of vulnerability is low, and in terms of the amount and distribution of precipitation, the risk of

Table 3 Statistics summary of COP maps

	C	O	P
Maximum	1	7	0.7
Minimum	0.18	1	0.7
Mean	0.41	4.6	0.7
SD	0.22	1.05	0

Table 2 Results of testing coliform bacteria in the springs of the studied area

Spring	The found bacteria
Dareh-e-Anari	*E. coli* (coliform bacteria)
	Entrobacter
	Klebsiella (coliform bacteria)
	Citrobacter
Abshekalo	*Entrobacter*
	Proteus mirabilis

Table 4 The statistical results of sensitivity analysis of one map removal using COP method

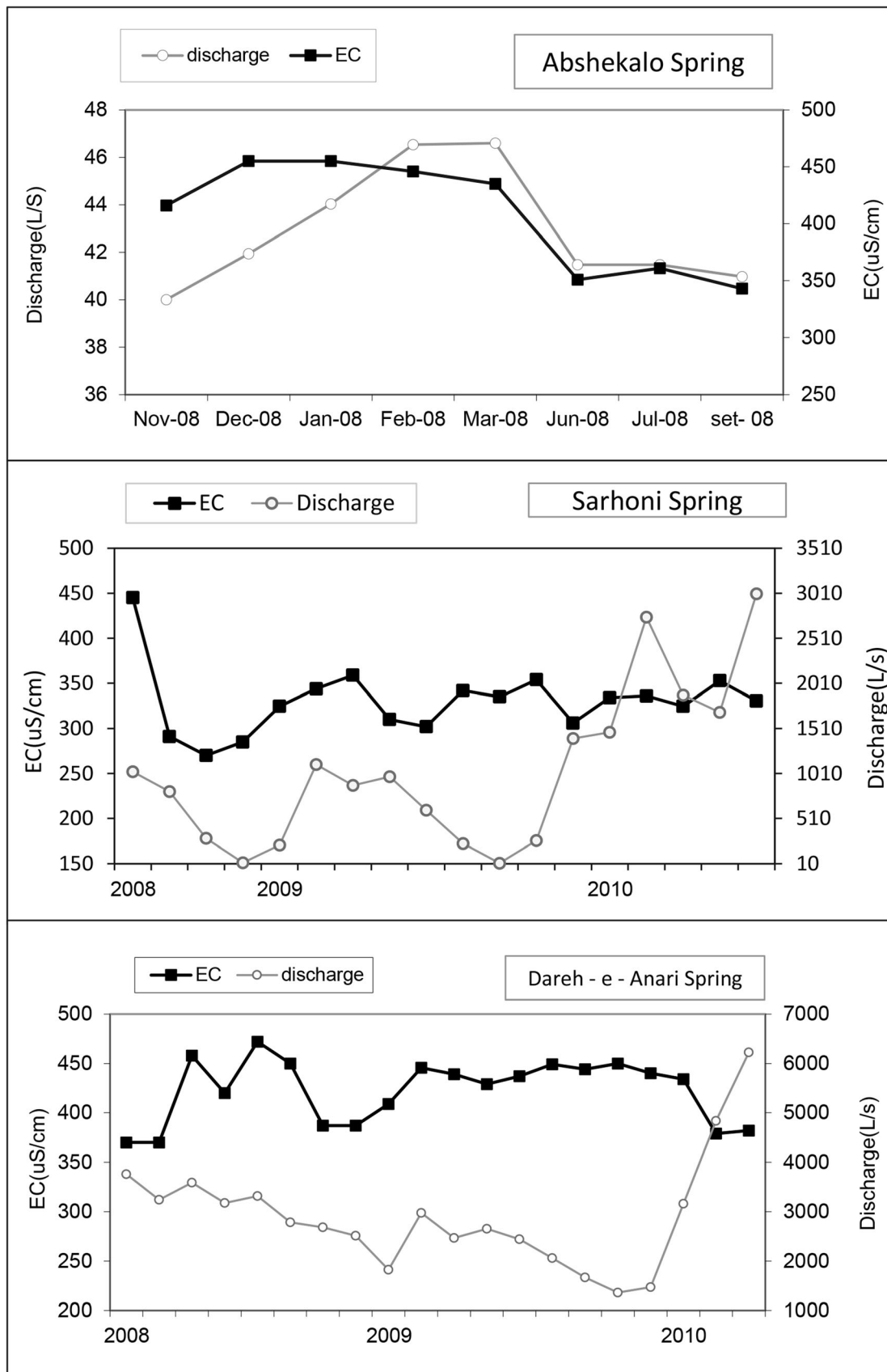| Removed parameter	Variation index (S%)			
	Mean	Max	Min	SD
C	122.6	322.22	0	74.98
O	21.8	26.2	8.33	3.15
P	38.1	109.52	2.38	1.43

Fig. 14 Comograph of Springs Dareh-e-Anari, Sarhoni, and Abshekaloin Shimbar karstic site

vulnerability is moderate. These results were validated and verified by using change of the water quality (hydraulic conductivity) in a short time after the changes in the debit of springs in areas with different vulnerability, and it was found that in Dareh-e-Anari and Sarhuni springs which located in the area of high vulnerability, the amount of hydraulic conductivity has decreased sharply in the short time after the increase in debit of springs, indicating the mixing of surface water with groundwater in a short period of time and a high vulnerability of the area, but in the case of Abshekalo Spring which is located in an area with medium vulnerability, reduction of dramatic EC is not significant and in a longer period of time occurs after increase of debit which indicates less vulnerability. Also, water of Dareh-e-Anari and Abshekalo springs was sampled as representatives of areas with high and medium vulnerabilities for testing coliform bacteria (indicating groundwater contamination by surface water), respectively. The results of the test showed that water of Dareh-e-Anari Spring has coliform bacteria, but Abshekalo Spring lacks these bacteria. This also confirms the obtained results. Therefore, this method has shown acceptable results in the studied area.

Compliance with ethical standards

Competing interests The authors declare that they have no competing interests.

Financial disclosure The authors declare that they have no financial disclosure.

References

Abshirini A (2004) Application of remote sensing techniques and GIS in identifying and potentiating the karst groundwater resources in Pabadeh-lali anticline. Unpublished M.A. thesis, Department of Remote Sensing and GIS, Shahid Chamran University of Ahvaz

Aller L, Bennet T, Leher JH, Petty RJ, Hackett G (1987). DRASTIC: a standardized system for evaluating ground water pollution potential using hydro-geological settings. EPA 600/2-87-035, 622

Andreo B, Ravbar N, Vías J (2009) Source vulnerability mapping in carbonate (karst) aquifers by extension of the COP method: application to pilot sites. Hydrogeol J 17(3):749–758

Biondic B, Bakalowicz M (1975) Hydrogeological aspects of groundwater protection in karstic areas. In: Cost action

Brouyère S et al (2001) Evaluation and validation of vulnerability concepts using a physically based approach. Mémoire des Sciences et Techniques de l'Environnement 13:67–72

Civita M (1994) Le carte della vulnerabilit'a degli acquiferi all'inquinamento: teoria e pratica [Contamination vulnerability mapping of the aquifer: theory and practice]. Quaderni di Tecniche di Protezione Ambientale, Pitagora Editrice

Daly D, Dassargues A, Drew D, Dunne S, Goldscheider N, Neale S, Popescu C, Zwhalen F (2002) Main concepts of the "European approach" for (karst) groundwater vulnerability assessment and mapping. Hydrogeol J 10(2):340–345

Davis A, Long A, Wireman M (2002) KARSTIC: a sensitivity method for carbonate aquifers in karst terrain. Environ Geol 42(1):65–72

Dimitriou E, Zacharias I (2006) Groundwater vulnerability and risk mapping in a geologically complex area by using stable isotopes, remote sensing and GIS techniques. Environ Geol 51(2):309–323

Doerfliger N, Zwahlen F (1998) Practical guide: groundwater vulnerability mapping in karstic regions (EPIK). Swiss Agency for the Environment, Forests and Landscape (SAEFL), Bern, p 56

Doerfliger N, Jeannin P-Y, Zwahlen F (1999) Water vulnerability assessment in karst environments: a new method of defining protection areas using a multi-attribute approach and GIS tools (EPIK method). Environ Geol 39(2):165–176

Fazeli M, Kalantari N, Rahimi MH, Khubyari A (2011) Investigating the spatial and temporal distribution of NO$_3$ contamination in groundwater resources of Zydoun Plain. J Water Eng 4:45–51

Ford D, Williams P (2013) Karst hydrogeology and geomorphology. John Wiley & Sons Ltd. https://doi.org/10.1002/9781118684986

Foster S (1987) Fundamental concepts in aquifer vulnerability, pollution risk and protection strategy. In: Duijvenbooden W, Van Waegeningh HG (eds) Vulnerability of soil and groundwater to pollutants. Committee on Hydrological Research, The Hague, pp 69–86

Goldscheider N)2004(The concept of groundwater vulnerability. In: Zwahlen F (ed) Vulnerability and risk mapping for the protection of carbonate (karst) aquifers, EUR 20912. Brussels7 European Commission, Directorate-General XII Science, Research and Development. p. 5–9

Goldscheider N, Popescu C (2004) The European approach. In: Zwahlen F (ed) Vulnerability and risk mapping for the protection of carbonate (karst) aquifers. European Commission, Brussels, pp 17–21

Goldscheider N, Klute M, Sturm S, Hötzl H (2000) The PI method—a GIS-based approach to mapping groundwater vulnerability with special consideration of karst aquifers. Z Angew Geol 46(3):157–166

Jeannin P-Y, Eichenberger U, Sinreich M, Vouillamoz J, Malard A, Weber E (2013) KARSYS: a pragmatic approach to karst hydrogeological system conceptualisation. Assessment of groundwater reserves and resources in Switzerland. Environ Earth Sci 69(3):999–1013

Kalantari N, Keshavarzi M, Hamidzadeh F, Sahebdel M (2010) Characteristics of heterogeneous Shimbar karstic systems in southwest Iran. In: Advances in Research in Karst Media. Springer, pp 69–74

Kavouri K, Plagnes V, Tremoulet J, Dörfliger N, Rejiba F, Marchet P (2011) PaPRIKa: a method for estimating karst resource and source vulnerability—application to the Ouysse karst system (southwest France). Hydrogeol J 19:339–353

Lodwick WA, Monson W, Svoboda L (1990) Attribute error and sensitivity analysis of map operations in geographical informations systems: suitability analysis. Int J Geogr Inf Syst 4(4):413–428

Malik P, Svasta J (1999) REKS-an alternative method of karst groundwater vulnerability estimation. In: Hydrogeology and Land Use Management. XXIX Congress of IAH, Bratislava, 1999, pp 79–85

Margat J (1968) Vulnerabilit'e des nappes d'eau souterraine `a la pollution [Contamination vulnerability mapping of groundwater]. Bureau de Recherches G'eologiques et Mini'eres, Orleans

Masoompour Samakosh J, Bagheri S, Davoodi M, Yarahmadi D, Jafari-Aghdam M, Soltani M (2013) Assessing and mapping the

vulnerability of karstic aquifer using gis and cop model. Glob NEST J 15(3):384–393

Moratalla Á, Gómez-Alday JJ, Sanz D, Castaño S, De Las Heras J (2011) Evaluation of a GIS-based integrated vulnerability risk assessment for the mancha oriental system (SE Spain). Water Resour Manag 25(14):3677–3697

Naghdizadegan Jahromi M, Ataeizadeh S, Mirzaei L, Alijani F (2013) Karst groundwater vulnerability assessment using cop method and analytic hierarchy process in Kamarderaz area, southwest Izeh. Second International Conference On Environmental Hazards, Tehran

Perrin J, Pochon A, Jeannin P-Y, Zwahlen F (2004) Vulnerability assessment in karstic areas: validation by field experiments. Environ Geol 46(2):237–245

Petelet-Giraud E, Dörfliger N, Crochet P (2000) RISKE: méthode d'évaluation multicritère de la vulnérabilité des aquifères karstiques. Application aux systèmes des Fontanilles et Cent-Fonts (Hérault, Sud de la France). Hydrogéologie 4:71–88

Plagnes V, Théry S, Fontaine L, Bakalowicz M, Dörfliger N (2005) Karst vulnerability mapping: improvement of the RISKE method. KARST 2005. Water resources and environmental problems in karst 14–19

Polemio M, Casarano D, Limoni PP (2009) Karstic aquifer vulnerability assessment methods and results at a test site (Apulia, southern Italy). Nat Hazards Earth Syst Sci 9(4):1461–1470

Ravbar N, Goldscheider N (2007) Proposed methodology of vulnerability and contamination risk mapping for the protection of karst aquifers in Slovenia. Acta Carsologica 36:397–411

Sha'bani M (2008) Determining the best geostatistic method in preparing the maps for changes in pH and groundwater TDS: a case study of Arasjan Plain. J Water Eng 1:47–58

Van Stempvoort D, Ewert L, Wassenaar L (1993) Aquifer vulnerability index (AVI): a GIS compatib method for groundwater vulnerability mapping. Can Water Res J 18:25–37

Vias J, Andreo B, Perles M, Carrasco F, Vadillo I, Jiménez P (2002) Preliminary proposal of a method for vulnerability mapping in carbonate aquifers. In: Second Nerja Cave Geol Symp Karst and Environment, 2002, Nerja, Spain, pp 20–23

Vías J, Andreo B, Perles M, Carrasco F, Vadillo I, Jiménez P (2006) Proposed method for groundwater vulnerability mapping in carbonate (karstic) aquifers: the COP method. Hydrogeol J 14(6):912–925

Vrba J, Zaporozec A (1994) Guidebook on mapping groundwater vulnerability. Heise, Hannover

Zwahlen F (ed) (2004) Vulnerability and risk mapping for the protection of carbonate (karst) aquifers, final report (COST action 620). European Commission, Brussels